



Contents lists available at ScienceDirect

Bioorganic & Medicinal Chemistry Letters

journal homepage: www.elsevier.com/locate/bmcl

Development of thioquinazolinones, allosteric Chk1 kinase inhibitors

Antonella Converso^{a,*}, Timothy Harting^a, Robert M. Garbaccio^a, Edward Tasber^a, Keith Rickert^b, Mark E. Fraley^a, Youwei Yan^c, Constantine Kretsoulas^a, Steve Stirdivant^b, Bob Drakas^b, Eileen S. Walsh^b, Kelly Hamilton^b, Carolyn A. Buser^b, Xianzhi Mao^b, Marc T. Abrams^b, Stephen C. Beck^b, Weikang Tao^b, Rob Lobell^b, Laura Sepp-Lorenzino^b, Joan Zugay-Murphy^c, Vinod Sardana^c, Sanjeev K. Munshi^c, Sylvie Marie Jezequel-Sur^d, Paul D. Zuck^d, George D. Hartman^a

^a Department of Medicinal Chemistry, Merck Research Laboratories, Merck & Co., P.O. Box 4, West Point, PA 19486, USA

^b Department of Cancer Research, Merck Research Laboratories, Merck & Co., P.O. Box 4, West Point, PA 19486, USA

^c Department of Structural Biology, Merck Research Laboratories, Merck & Co., P.O. Box 4, West Point, PA 19486, USA

^d Department of Automated Biotechnology, Merck Research Laboratories, Merck & Co., P.O. Box 4, West Point, PA 19486, USA

ARTICLE INFO

Article history:

Received 15 October 2008

Revised 16 December 2008

Accepted 17 December 2008

Available online 24 December 2008

Keywords:

Chk1

Thioquinazolinone

Allosteric kinase inhibitor

X-ray crystal structure

ABSTRACT

A high throughput screening campaign was designed to identify allosteric inhibitors of Chk1 kinase by testing compounds at high concentration. Activity was then observed at K_m for ATP and at near-physiological concentrations of ATP. This strategy led to the discovery of a non-ATP competitive thioquinazolinone series which was optimized for potency and stability. An X-ray crystal structure for the complex of our best inhibitor bound to Chk1 was solved, indicating that it binds to an allosteric site ~ 13 Å from the ATP binding site. Preliminary data is presented for several of these compounds.

© 2009 Elsevier Ltd. All rights reserved.

Despite decades of research towards the identification of an anticancer drug devoid of serious side-effects, DNA damaging agents are still one of the most relied upon cancer therapeutics in the clinic due to their efficacy. Such agents often present a limited therapeutic window and/or poor selectivity for cancer cells over normal cells. Thus, any improvement in their efficacy is extremely valuable. Recently, it has been suggested that the inhibition of checkpoint kinase Chk1 may offer such an opportunity.

Chk1 and the tumor suppressor protein *p53* protect cells that have suffered DNA damage by arresting the cell cycle to allow DNA repair.^{1–3} Importantly, 50–70% of tumor cells have defects in their *p53* DNA damage response pathway and must rely exclusively on Chk1 for DNA repair and cell survival. Inhibition of Chk1 will therefore abrogate repair from DNA damage in *p53* defective tumors, ultimately resulting in premature progression into mitosis and apoptosis. Normal cells, on the other hand, can still repair via *p53*-mediated arrest. As a result, Chk1 inhibitors should sensitize *p53*-deficient cancer cells to DNA damaging agents without enhancing toxicity toward non-malignant cells. As such, Chk1 inhibitors⁴ have the potential to widen the therapeutic window for DNA damaging agents in *p53*-deficient tumors.

Chk1 is one of 518 kinases encoded by the human genome.⁵ Kinases are ubiquitous and important for a variety of physiological as well as pathological cellular processes.⁶ They are characterized by a highly conserved ATP-binding hinge region which is the traditional site targeted to block the activity of these enzymes. An alternative approach has involved the identification of inhibitors that bind outside of the catalytic cleft at an allosteric site. These allosteric inhibitors are non-ATP competitive and, due to the variability—or absence—of the allosteric site, they may offer an advantage when trying to modulate kinases selectively.

The Chk1-targeted program at Merck has been prevalently focused on the development of ATP competitive inhibitors⁷ and facilitated by known Chk1 structural data. However, fine tuning of leads to exclude activity towards other kinases has proven difficult. For this reason we prioritized the identification of allosteric leads and developed a screening strategy that could be useful towards the future discovery of non-ATP competitive kinase inhibitors. To this end, a multi-step homogenous time-resolved fluorescence (HTRF) assay suitable for high throughput screen was implemented in 1536-well plate format.⁸

Under the assumption that allosteric leads may have low affinity, we chose to screen at high compound concentration (50 μ M). Hits were then evaluated in the presence of ATP at K_m and at physiological ATP concentration (0.1 and 2.0 mM) in order to eliminate ATP-com-

* Corresponding author. Tel.: +1 215 652 4856; fax: +1 215 652 7310.
E-mail address: antonella_converso@merck.com (A. Converso).

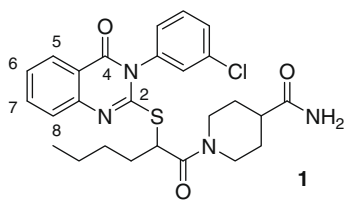


Figure 1. Chk1 inhibitor lead 1.

petitive compounds: the potency of allosteric inhibitors should be insensitive to ATP concentration. A single lead, thioquinazolinone **1** (see Fig. 1), was identified from this effort with an IC_{50} of 17 and 24 μM at 0.1 and 2.0 mM ATP concentration, respectively.

Thioquinazolinone **1** constituted the starting point for our lead optimization effort. Analogs of **1** were prepared using the general reaction sequence shown in Scheme 1.⁹

Anthranilic acid **2** was reacted with aromatic and aliphatic isothiocyanates to give mercapto-quinazolines **3** in 80–95% yield. Alkylation of the thiol in **3** with a variety of α -bromo acids afforded **4**, which was then coupled with a variety of amines to yield thioquinazolinone amides **5**.

Medicinal chemistry efforts began by varying the R^4 and R^5 groups on the terminal amide, which was conveniently introduced at the end of the synthesis for this series. Analogues synthesized demonstrated tight SAR (Table 1). It was generally found that a fully substituted amide is necessary for potency. Ethyl esters were inactive against Chk1¹¹ (data not shown), and so were primary amides (compounds **7–10**). Piperazines and piperidines enhanced potency with compounds **11** and **13** providing the greatest potency with IC_{50} of 3 μM . Diphenylpiperidine **14**, while moderately potent, showed poor solubility, and sulfonamide **12** suffered from stability issues. Neither was pursued further.

We then investigated the R^3 group on the mercaptoquinazolinone carboxylic acid. To this end, the aromatic thiol was reacted with a variety of α -bromo acids, followed by coupling to piperidine-4-carboxamide (Table 2).

The aromatic analogue **16** derived from α -bromophenylacetic acid presented similar activity as the original lead giving an IC_{50} of 21 μM . Branching at the β -position renders the corresponding thioquinazolinone inactive (**15**), while γ -branching as in compound **17** gave a sixfold improvement in potency. However, the combination of the best amide in **13** with this R^3 group did not lead to further potency gains. Interestingly, we observed acid-instability issues when we removed the R substituent altogether: the final amide coupling appeared to be successful, but removal of the acidic solvent mixture after reverse-phase HPLC separation gave

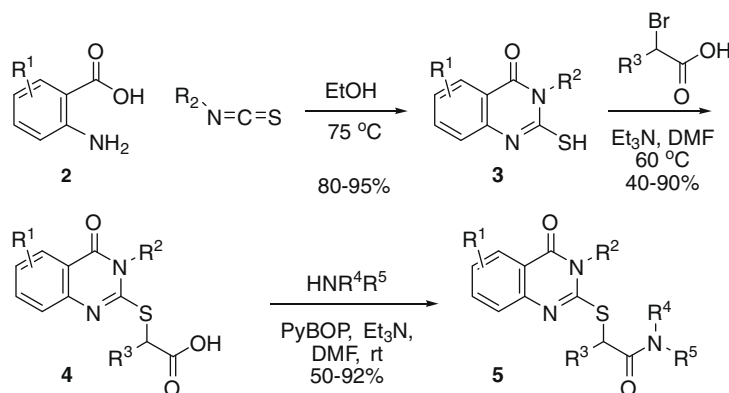
Table 1

Chk1 inhibition data for thioquinazolinone amides **1–14**

Compound	NR^4R^5	SL Chk1 IC_{50} 0.1 mM ATP (μM)
1		17
6		Max inh. 62% @ 100 μM
7		>100
8		>100
9		>100
10		Max inh. 3% @100 μM
11		3.3
12		6.0
13		3.8
14		4.5

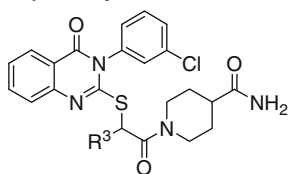
complete and clean decomposition to carboxylic acid **4** even at room temperature.

We next turned our attention to the aromatic ring on the thioquinazolinone core and the internal thioquinazolinone amide substituent R^2 introduced in the first synthetic step. Coupling of anthranilic acid with a variety of isothiocyanates allows variation of the R^2 group as reported in Table 3. Again, SAR proved to be



Scheme 1. Synthesis of thioquinazolinones. Detailed synthetic procedures can be found in Ref. 10.

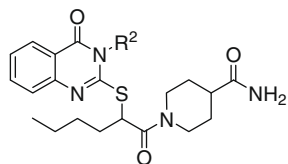
Table 2
Effect of R³ on Chk1 potency of thioquinazolinones



Compound	R ³	SL Chk1 IC ₅₀ 0.1 mM ATP (μM)
1		17
15		>100
16		21
17		2.8

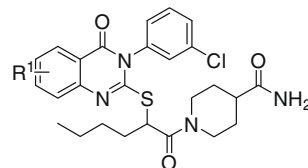
tight: the aromatic residue was necessary for activity, with all aliphatic thioquinazolinones synthesized showing low activity and poor stability, rapidly decomposing to carboxylic acid **4** in the presence of diluted aqueous TFA (compounds **18–20**). Substitution on the aryl ring in R² was then examined and a chlorine scan showed that the starting *meta* position was optimal for activity (compounds **21–22**). Introduction of heterocycles either attached directly to the amide nitrogen (**23** and **24**) or separated by a methylene unit (**25**) caused a loss in potency.

Table 3
Effect of R² groups on Chk1 potency of thioquinazolinones



Compound	R ²	SL Chk1 IC ₅₀ 0.1 mM ATP (μM)
18		Max inh. 17% @ 100 μM
19		Max inh. 20% @ 100 μM
20		Max inh. 48% @ 100 μM
21		41
1		17
22		>100
23		Max inh. 35% @ 100 μM
24		Max inh. 20% @ 100 μM
25		Max inh. 26% @ 100 μM

Table 4
Effect of thioquinazolinone ring substitution on potency



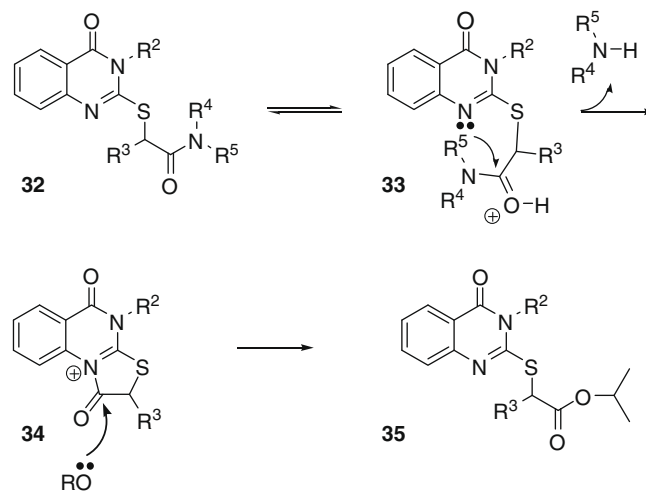
Compound	R ¹	SL Chk1 IC ₅₀ 0.1 mM ATP (μM)
26	5-Me	>100
27	6-Me	Max inh. 30% @ 100 μM
28	7-Me	28
29	8-Me	17
30	8-OH	20
31	8-OMe	21

Substituents R¹ on the aromatic region of the thioquinazolinone were then examined (Table 4). Introduction of a methyl group at positions 5 and 6 was not tolerated, while methyl substitution at positions 7 and 8 had little to no effect on the IC₅₀. A wide range of different substituents at C7 and C8 (data not shown) was therefore studied, in the hopes of increasing potency. While potency decreased following substitution at C7, substitution at the 8-position had virtually no effect.

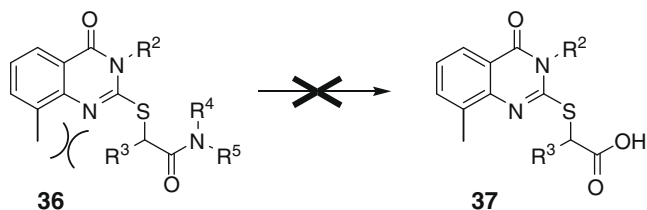
While investigating the SAR for the series, we also focused on addressing its stability issues. We observed thioquinazolinone decomposition in three specific instances: (1) for certain amides; (2) when lacking R³ substitution on the sulfur-containing side chain, and (3) in the presence of electron rich R² groups. In all cases we obtained clean conversion to the starting carboxylic acid **4**. Examination of the experimental data led us to propose that the N1 lone pair in the thioquinazolinone is involved in intramolecular amide decomposition as depicted in Scheme 2.

Formation of charged intermediate **33** is consistent with our observations for a couple of reasons. First, when R³ = H, the carbonyl carbon is less hindered towards nucleophilic attack. Secondly, an alkyl rather than aryl R² group renders the thioquinazolinone more electron rich so that the N1 lone pair is more nucleophilic, resulting in accelerated decomposition. In further support of the proposed mechanism, we were able to trap **34** with isopropanol, which provided the corresponding isopropyl ester.

Our previous work at C8 of the thioquinazolinone ring showed that potency in this series is independent of C8 substitution. At the



Scheme 2. Proposed mechanism for the decomposition of thioquinazolinones.



Scheme 3. Effect of C8 substituent on the decomposition of **36**.

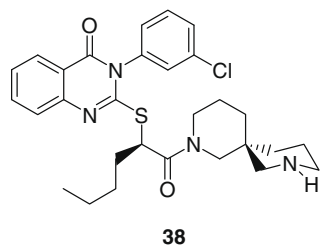


Figure 2. Active diastereomer of thioquinazolinone mixture **13**. $IC_{50} = 1.3 \mu M$.

same time, a substituent at C8 has the maximum impact on the steric environment of the nucleophilic N1 nitrogen. If our hypothesis for the observed decomposition is correct, shielding of the N1 lone pair by the introduction of a vicinal methyl should impart robustness to the central core by preventing intramolecular nucleophilic attack (Scheme 3). Our hypothesis was nicely confirmed by stability studies performed on **36**, the 8-Me analogue of compound **13**, which, unlike **13** did not decompose in concentrated aqueous TFA even after several days.

As part of our medicinal chemistry efforts, we separated **13** ($IC_{50} = 3 \mu M$) into its four diastereomers and we found that only the (*S,S*) diastereomer **38** (Fig. 2) binds to Chk1 with an IC_{50} of 1.3 μM , with all the others being inactive in our assay.

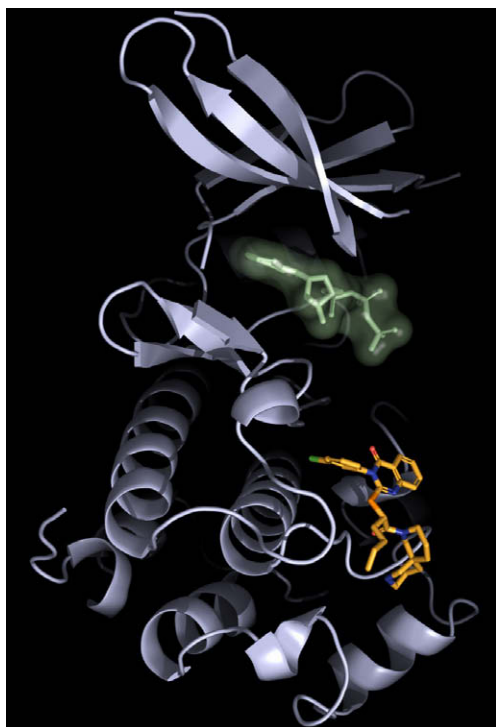


Figure 3. Compound **38** (gold) bound to Chk1. ATP (semitransparent gray) from 1PHK¹² used to orient the reader.

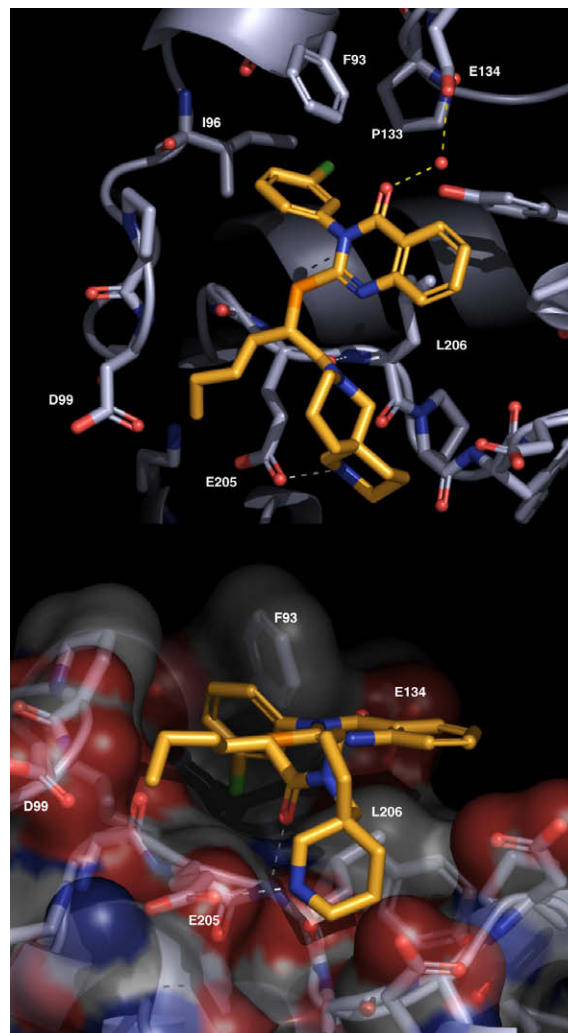


Figure 4. Two perspectives of **38** (gold) bound to Chk1. Direct hydrogen bonding contacts to the carboxylic acid of Glu205 and the backbone amide nitrogen of Leu206 are shown in white dashes. Water mediated hydrogen bond to Glu134 is shown as a yellow dash. The *p*-chlorophenyl quinazolinone occupies a hydrophobic pocket formed by Phe93, Ile96, Pro133, and Leu206, forming a π - π interaction.

Satisfyingly, we were also able to obtain a crystal structure of diastereomerically pure **38** bound to a truncated version of Chk1¹³ (Fig. 3).

The structure clearly confirms **38** as an allosteric inhibitor, binding $\sim 13 \text{ \AA}$ from ATP and its pocket in a shallow hydrophobic region on the surface of the enzyme. The spiro-piperidine amine is engaged in two direct hydrogen bonding contacts with the carboxylic acid of Glu205 and the backbone amide nitrogen of Leu206 (white dashes in Fig. 4). The thioquinazolinone carbonyl oxygen participates in a water mediated hydrogen bond to Glu134 (yellow dash in Fig. 4).

The crystal structure is consistent with the medicinal chemistry results obtained in our series. The aromatic ring at R² slides into a very narrow hydrophobic cleft that wraps it tightly. Serendipitously, the initial *meta*-chloro substitution on R² appears optimal in terms of size and lipophilicity.

The lack of sensitivity to substitution at the C-8 position of the thioquinazolinone can now be rationalized by the fact that **38** binds *on the surface* of the enzyme, and that the thioquinazolinone aromatic core overlaps with a very hydrophobic region on it. Any small substituent on the thioquinazolinone ring is out of reach of hydrogen bond acceptors or donors on the enzyme that could stabilize its interaction with **38**.

As the crystal structure for **38** reveals, the thioquinazolinones bind to the enzyme in a highly solvent-exposed fashion. The necessary desolvation energy may not be well compensated by these limited interactions with the enzyme and might explain the low potencies shown by this series.

Thioquinazolinone **38** and its active analogues present a markedly different selectivity profile compared to ATP-competitive Chk1 inhibitors previously synthesized in our laboratories. A more in-depth discussion of this aspect of binding, together with full biochemical characterization of the complex inhibition mode of this series, will be reported in a separate publication.

In summary, a series of thioquinazolinone allosteric Chk1 inhibitors were discovered by an appropriately targeted HTS campaign designed for the identification of weak, non-ATP competitive leads. An efficient synthetic route has been developed to facilitate the SAR studies. We identified stability issues with some members of this series, a mechanism for the decomposition and a way to prevent it. Additional efforts have resulted in the solution of the first crystal structure of an inhibitor bound to the allosteric site of the Chk1 enzyme.

Supplementary data

Supplementary data associated with this article can be found, in the online version, at doi:10.1016/j.bmcl.2008.12.076.

References and notes

- (a) Zhou, B. B.; Bartek, J. *Nat. Rev. Cancer* **2004**, *4*, 1; (b) Bartek, J.; Lukas, J. *Cancer Cell* **2003**, *3*, 421.
- Kong, N.; Fotouhi, N.; Wovkulich, P. M.; Roberts, J. *Drugs Future* **2003**, *28*, 881.
- Kawabe, T. *Mol. Cancer Ther.* **2004**, *3*, 513.
- (a) Prudhomme, M. *Recent Patents on Anti-Cancer Drug Discovery* **2006**, *1*, 55; (b) Cho, S. H.; Toouli, C. D.; Fujii, G. H.; Crain, C.; Parry, D. *Cell cycle* **2005**, *4*, 131; (c) Luo, Y.; Rockow-Magnone, S. K.; Joseph, M. K.; Bradner, J.; Butler, C. C.; Tahir, S. K.; Han, E. K.-H.; Ng, S.-C.; Severin, J. M.; Gubbins, E. J.; Reilly, R. M.; Rueter, A.; Simmer, R. L.; Holzman, T. F.; Giranda, V. L. *Anticancer Res.* **2001**, *21*, 23; (d) Koniaras, K.; Cuddihy, A. R.; Christopoulos, H.; Hogg, A.; O'Connell, M. J. *Oncogene* **2001**, *20*, 7453; (e) Maude, S. L.; Enders, G. H. *Cancer Res.* **2005**, *65*, 780; (f) Hattori, H.; Kuroda, M.; Ishida, T.; Shinmura, K.; Nagai, S.; Mukai, K.; Imakiire, A. *Pathol. Int.* **2004**, *54*, 26; (g) Blagden, S.; de Bono, J. *Current Drug Targets* **2005**, *6*, 325; (h) Chen, Z.; Xiao, Z.; Gu, W.-Z.; Xue, J.; Bui, M. H.; Kovar, P.; Li, G. n.; Wang, G.; Tao, Z.-F.; Tong, Y.; Lin, N.-H.; Sham, H. L.; Wang, J. Y. J.; Sowin, T. J.; Rosenberg, S. H.; Zhang, H. *Int. J. Cancer* **2006**, *119*, 2784.
- Manning, G.; Whyte, D. B.; Martinez, R.; Hunter, T.; Sudarsanam, S. *Science* **2002**, *298*, 1912.
- (a) Weinmann, H.; Metternich, R. *ChemBioChem* **2005**, *6*, 1; (b) Woodgett, J. *Protein Kinase Functions; Front. Mol. Biol.* **2000**, *29*, 1.
- (a) Fraley, M. E.; Steen, J. T. PCT Int. Appl. WO 2007015837, 2007.; (b) Arrington, K. L.; Dudkin, V. Y.; Fraley, M. E.; Garbaccio, R. M.; Hartman, G. D.; Huang, Y.; Kretsoulas, C.; Tasber, E. S., PCT Int. Appl. WO 2007008502, 2007.; (c) Arrington, K. L.; Fraley, M. E.; Garbaccio, R. M.; Huang, S. Y.; Lindsley, C. W.; Steen, J. T.; Yang, F. PCT Int. Appl. WO 2006086255, 2006.; (d) Brnardic, E. J.; Fraley, M. E.; Garbaccio, R. M.; Steen, J. T. PCT Int. Appl. WO 2006074281, 2006.; (e) Fraley, M. E.; Steen, J. T.; Brnardic, E. J.; Arrington, K. L.; Spencer, K. L.; Hanney, B. A.; Kim, Y.; Hartman, G. D.; Stirdivant, S. M.; Drakas, B. A.; Rickert, K.; Walsh, E. S.; Hamilton, K.; Buser, C. A.; Hardwick, J.; Tao, W.; Beck, S. C.; Mao, X.; Lobell, R. B.; Sepp-Lorenzino, L.; Yan, Y.; Ikuta, M.; Munshi, S. K.; Kuo, L. C.; Kretsoulas, C. *Bioorg. Med. Chem. Lett.* **2006**, *23*, 6049; (f) Huang, S.; Garbaccio, R. M.; Fraley, M. E.; Steen, J.; Kretsoulas, C.; Hartman, G.; Stirdivant, S.; Drakas, B.; Rickert, K.; Walsh, E.; Hamilton, K.; Buser, C. A.; Hardwick, J.; Mao, X.; Abrams, M.; Beck, S.; Tao, W.; Lobell, R.; Sepp-Lorenzino, L.; Yan, Y.; Ikuta, M.; Murphy, J.; Sardana, V.; Munshi, S.; Kuo, L.; Reilly, M.; Mahan, E. *Bioorg. Med. Chem. Lett.* **2006**, *22*, 5907.
- In the first step, Chk1 enzyme was incubated with ATP and biotin-labeled GSK3 α peptide. In the second step the sample was treated with monoclonal anti-phospho-GSK3 α peptide antibody labeled with europium (Eu³⁺) (Eu-Ab) and streptavidin (SA) linked to XL665 (SA-XL665). The Eu-Ab antibody recognizes the phosphoserine residue of GSK3 α peptide, whereas SA-XL665 binds to the biotin at the N-terminus of the peptide. This ternary complex (biotin-phosphorylated GSK3 α /Eu-Ab/SA-XL665) was then detected by excitation of Eu³⁺ at 337 nm, fluorescence resonance energy transfer (FRET) from Eu³⁺ to XL665, and fluorescence emission from XL665 at 665 nm. In this assay, an inhibitor of Chk1 enzyme could be detected by a decrease of fluorescence.
- Bhargava, P. R.; Ram, P. *Bull. Chem. Soc. Jpn.* **1967**, *38*, 342.
- Representative experimental procedure: 3-Alkyl-2-sulfanylquinazolin-4(3H)-one **3**: Anthranilic acid **2** was dissolved in EtOH (0.5 M) and heated to 75 °C. The isothiocyanate (2 equiv) was added in 0.5 equiv portions over the course of 8 h until disappearance of anthranilic acid. The mixture was cooled, and the slurry was filtered and washed with cold ethanol to afford pure 2-mercaptoquinazolin-4(3H)-one **3**. Thioquinazolinone **5**: 3-Alkyl-2-sulfanylquinazolin-4(3H)-one **3**, α -bromoacid (1.3 equiv) and triethylamine (6 equiv) were dissolved in anhydrous DMF (0.5 M) and stirred at 75 °C until LC-MS indicated disappearance of starting material to yield 3-alkyl-2-[(3-methyl-4-oxo-3,4-dihydroquinazolin-2-yl)sulfanyl] acid **4**. The reaction mixture was cooled, and triethylamine (3 equiv), the amine (2 equiv), and PyBOP (2 equiv) were added. Once LC-MS showed that the reaction was complete, the reaction mixture was filtered and purified with reverse-phase HPLC (H₂O/CH₃CN gradient w/0.1% TFA present) to yield pure product **5**.
- Chk1 inhibitory activity was measured using a homogenous time-resolved fluorescence assay which measures phosphorylation of a biotinylated GSK-3 peptide as described in Barnett et al. *Biochem. J.* **2005**, *385*, 399. For the construct, a naturally occurring exon 10 splice variant of human Chk1 described in patent application US20050266469(A1), containing primarily the kinase domain, was expressed in baculovirus with a C-terminal 6-histidine tag. This protein was purified on a Ni affinity column and used as is for kinetic assays, or purified further on Heparin and SEC columns for crystallography. The Chk1 concentration was 0.5 nM and ATP was used at 0.1 mM. IC₅₀ values are reported as the averages of at least two independent determinations; standard deviations are within ± 25 –50% of IC₅₀ values.
- Compound **38** was diffused into pre-formed apo Chk1 kinase domain crystals by the soaking method. The X-ray diffraction data were collected from these Chk1 inhibitor complex crystals to 1.9 Å, resolution with $R_{\text{sym}} = 0.066$ and completeness = 98%, respectively. The complex structures were refined to an R-factor of 0.182. The chlorobenzene ring of compound **38** has two conformations at 70% and 30% occupancies, respectively. The detailed X-ray diffraction data and refinement statistics are listed under PDB code 3F9N at the protein data bank. The crystallographic parameters are reported in the supporting information for this article.
- Owen, D. J.; Noble, M. E.; Garman, E. F.; Papageorgiou, A. C.; Johnson, L. N. *Structure* **1995**, *3*, 467.